

Supporting Information

Performance Optimization and Fast Rate Capabilities of Novel Polymer Cathode Materials through Balanced Electronic and Ionic Transport

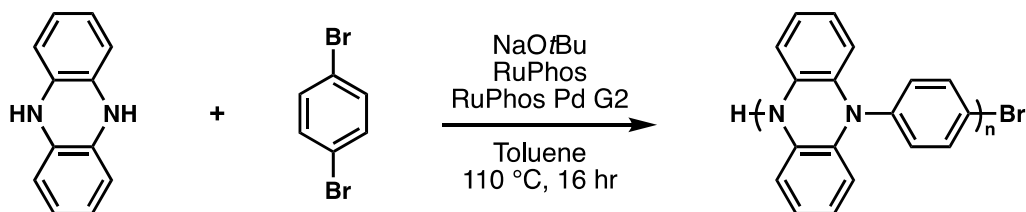
Cara N. Gannett, Brian M. Peterson, Luis Melecio-Zambrano, Colleen Q. Trainor, Brett P. Fors*, and Héctor D. Abruña*

Experimental Information

General Reagent Information

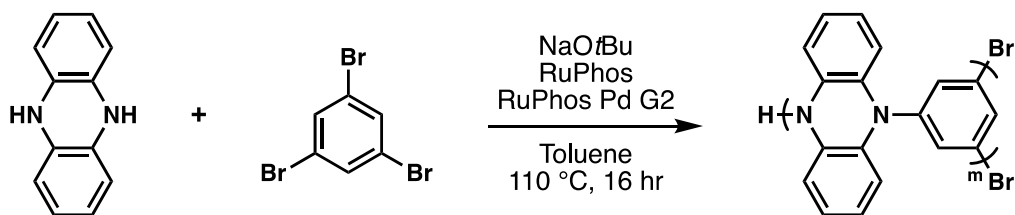
Toluene and dichloromethane (DCM) were purchased from J.T. Baker and purified by vigorous purging with argon for 2 hours, followed by passing through two packed columns of neutral alumina under argon pressure. RuPhos (95%), RuPhos Pd G2, and sodium *tert*-butoxide (NaOtBu) were purchased from Millipore Sigma and used as received. Phenazine (99%) and 1,4-dibromobenzene (98%) were purchased from Alfa Aesar and used as received. Sodium dithionite was purchased from Oakwood Chemicals and used as received. 1-Methyl-2-pyrrolidinone (NMP) (anhydrous 99.5%) was purchased from Sigma-Aldrich and used as received. CMK-3, ordered mesoporous carbon was purchased from ACS materials and used as received. Super P carbon (Imerys Graphite& Carbon) and poly(vinylidene fluoride) (PVDF) (Kynar Flex) were dried overnight in a vacuum oven at 60 °C before use. Electrolyte components, EC (ethylene carbonate) (99+%), DEC (diethyl carbonate) (99+%), and LiPF₆ (98+%) were purchased from Aldrich and stored in an argon filled glovebox.

Synthesis of co-polymers



Synthesis of poly(Ph-PZ)

A Schlenk tube was charged with 5,10-dihydrophenazine (273 mg, 1.5 mmol, 1 equiv), 1,4-dibromobenzene (354 mg, 1.5 mmol, 1 equiv), sodium *tert*-butoxide (317 mg, 3.3 mmol, 2.2 equiv), RuPhos Pd G2 (11 mg, 0.015 mmol, 0.01 equiv), and RuPhos ligand (7 mg, 0.015 mmol, 0.01 equiv). The Schlenk tube was then evacuated, backfilled with nitrogen, and toluene (5 mL) was added. The reaction was stirred at 110 °C for 16 hours. After the reaction cooled, the reaction mixture was suspended in dichloromethane (100 mL), vortexed, and washed with water (100 mL) five times, or until all sodium bromide was removed by powder x-ray diffraction. After filtration, the polymer was dried under vacuum, yielding a light brown powder (360 mg). IR (ATR, cm⁻¹): $\nu = 3052, 1603, 1503, 1475, 1456, 1329, 1261, 1158, 1062, 1015, 924, 817, 723, 620, 560$. Elemental Anal. Found: C, 81.49; H, 4.61; N, 10.28; Br, 0.97.

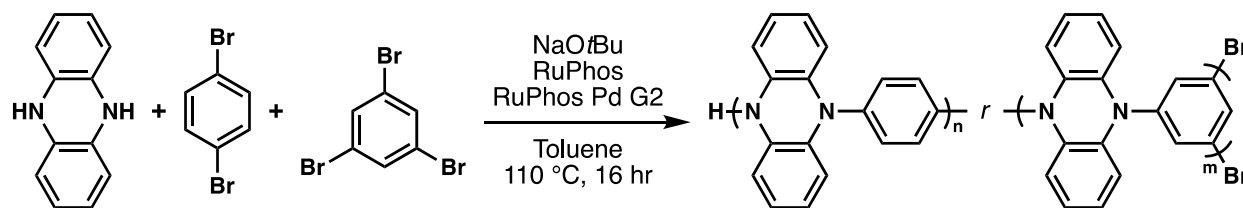


Synthesis of poly(135Ph-PZ)

A Schlenk Tube was charged with 5,10-dihydrophenazine (273 mg, 1.5 mmol, 1 equiv), 1,3,5-tribromobenzene (315 mg, 1.0 mmol, 0.66 equiv), sodium *tert*-butoxide (346 mg, 3.6 mmol, 2.4 equiv), RuPhos Pd G2 (16 mg, 0.02 mmol, 0.01 equiv), and RuPhos ligand (9.3 mg, 0.02 mmol, 0.01 equiv). The Schlenk tube was evacuated, backfilled with nitrogen, and toluene (5 mL) was added. The reaction was stirred at 110 °C for 16 hours. After the reaction cooled, the reaction mixture was suspended in dichloromethane (100 mL), vortexed, and washed with water (100 mL) five times, or until all sodium bromide was removed by powder x-ray diffraction. After filtration, the polymer was dried

under vacuum, yielding a brown powder (312 mg) IR (ATR, cm^{-1}): $\nu = 3056, 1575, 1475, 1439, 1322, 1280, 1250, 1144, 1012, 930, 846, 730, 705, 620, 566$. Elemental Anal. Found: C, 77.87; H, 4.28; N, 10.90; Br, 2.01.

Synthesis of ter-polymers



General Procedure

5,10-dihydrophenazine, 1,4-dibromobenzene, 1,3,5-tribromobenzene, sodium *tert*-butoxide, RuPhos Pd G2, and RuPhos ligand were charged to a Schlenk tube. A nitrogen atmosphere was established, and toluene (5 mL) was added. The reaction was stirred at 110 °C for 16 hours. The reaction was cooled, suspended in dichloromethane (100 mL), and washed with water (100 mL) five times, or until all sodium bromide was removed by powder x-ray diffraction.

Synthesis of poly(135Ph-PZ)-10

The general procedure was followed employing 5,10-dihydrophenazine (182 mg, 1 mmol, 1 equiv), 1,4-dibromobenzene (132 mg, 0.9 mmol, 0.9 equiv), 1,3,5-tribromobenzene (21 mg, 0.07 mmol, 0.07 equiv), sodium *tert*-butoxide (231 mg, 2.4 mmol, 2.4 equiv), RuPhos Pd G2 (16 mg, 0.02 mmol, 0.02 equiv), and RuPhos ligand (9 mg, 0.02 mmol, 0.02 equiv). The polymer (255 mg) was obtained as a light brown powder. IR (ATR, cm^{-1}): $n = 3052, 1603, 1581, 1503, 1475, 1456, 1329, 1280, 1261, 1093, 1062, 1015, 926, 817, 723, 620, 560$. Elemental Anal. Found: C, 76.81; H, 4.44; N, 9.91; Br, 4.08.

Synthesis of poly(135Ph-PZ)-25

The general procedure was followed employing 5,10-dihydrophenazine (182 mg, 1 mmol, 1 equiv), 1,4-dibromobenzene (177 mg, 0.75 mmol, 0.75 equiv), 1,3,5-tribromobenzene (52 mg, 0.17 mmol, 0.17 equiv), sodium *tert*-butoxide (231 mg, 2.4 mmol, 2.4 equiv), RuPhos Pd G2 (16 mg, 0.02 mmol, 0.02 equiv), and RuPhos ligand (9 mg, 0.02 mmol, 0.02 equiv). The polymer (210 mg) was obtained as a light brown powder. IR (ATR, cm^{-1}): $n = 3052, 1603, 1581, 1503, 1475, 1456, 1329, 1280, 1261, 1093, 1157, 1062, 1015, 926, 910, 817, 723, 620, 560$. Elemental Anal. Found: C, 79.47; H, 4.56; N, 10.47; Br, 1.75.

Synthesis of poly(135Ph-PZ)-50

The general procedure was followed employing 5,10-dihydrophenazine (182 mg, 1 mmol, 1 equiv), 1,4-dibromobenzene (118 mg, 0.5 mmol, 0.5 equiv), 1,3,5-tribromobenzene (105 mg, 0.33 mmol, 0.33 equiv), sodium *tert*-butoxide (231 mg, 2.4 mmol, 2.4 equiv), RuPhos Pd G2 (16 mg, 0.02 mmol, 0.02 equiv), and RuPhos ligand (9 mg, 0.02 mmol, 0.02 equiv). The polymer (183 mg) was obtained as a brown powder. IR (ATR, cm^{-1}): $n = 3052, 1677, 1603, 1581, 1503, 1475, 1456, 1329, 1280, 1250, 1157, 1062, 1015, 926, 910, 821, 730, 620, 560$. Elemental Anal. Found: C, 78.79; H, 4.42; N, 10.56; Br, 2.20.

Synthesis of poly(135Ph-PZ)-75

The general procedure was followed employing 5,10-dihydrophenazine (182 mg, 1 mmol, 1 equiv), 1,4-dibromobenzene (59 mg, 0.25 mmol, 0.25 equiv), 1,3,5-tribromobenzene (157 mg, 0.5 mmol, 0.5 equiv), sodium *tert*-butoxide (231 mg, 2.4 mmol, 2.4 equiv), RuPhos Pd G2 (16 mg, 0.02 mmol, 0.02 equiv), and RuPhos ligand (9 mg, 0.02 mmol, 0.02 equiv). The polymer (173 mg) was obtained as a dark brown powder. IR (ATR, cm^{-1}): $n = 2981, 1575, 1475, 1456, 1439, 1322, 1280, 1250, 1156, 1012, 930, 910, 821, 730, 620$. Elemental Anal. Found: C, 81.66; H, 4.44; N, 11.19; Br, 0.48.

Coin Cell Fabrication

The polymers were studied for their electrochemical properties using CR 2032 Li metal half cells. The cathode was constructed by mixing a composite of 60 % active material, 15% Super P carbon, 15% CMK-3 mesoporous carbon, and 10% PVDF binder (percentages by weight) in NMP. For the high active mass ratio cells, 80% active material was mixed with 5% Super P carbon, 5% CMK-3 mesoporous carbon, and 10% PVDF binder in the slurry composite. First, the binder was dissolved in a small volume of NMP by mixing with a mortar and pestle, followed by the incorporation of the conductive carbon, and then the active material. Additional NMP was added in small volumes during mixing to create the consistency of a thick ink. The slurry was thoroughly mixed for 20 minutes, to ensure homogeneity. The homogeneous mixture was coated onto a carbon paper current collector (Fuel Cell Store) using the doctor blade method. The electrode composite was dried in a vacuum oven for 2 hours at 60°C followed by 110°C overnight. The dried electrode was cut into disks for assembly into coin cells. Disks of 3/16" diameter were used for CV tests to reduce the effect of iR drop, while disks 3/8" in diameter were used for GITT and galvanostatic charge/discharge experiments. The half cells were assembled in an argon filled glovebox with less than 0.50 ppm O₂. Li metal foil (Alfa Aesar, 0.75 mm, 99.9%) was punched into 9/16" disks as the anode and dried glass microfiber filters (GF/A, Whatman) were used as separators. For the electrolyte solution, 80 μL of 1 M LiPF₆ in EC:DEC (1:1 by volume) was used. Once sealed, the cells were removed from the glovebox for electrochemical testing. The active mass loading per geometric area was approximately 0.7 mg/cm² and 0.9 mg/cm², for cells with 60% and 80% active material in the cathode composite, respectively. Active mass per geometric area varied from cell to cell due to the nature of the carbon paper current collector.

Galvanostatic Intermittent Titration Technique (GITT)

Using a Neware battery test station, GITT measurements were performed on assembled coin cells over a charge/discharge cycle. Before performing GITT, each cell was cycled three times at 0.1 A g⁻¹. Following the third cycle, a three-minute constant current charging pulse of 0.1 A g⁻¹ was applied to the cell followed by an hour of rest to allow for the cell to reach equilibrium. This step was repeated until the cell's equilibrium voltage was greater than the upper voltage cutoff (4.0 V vs. Li/Li⁺ for poly(Ph-PZ), poly(135Ph-PZ)-10, poly(135Ph-PZ)-25; 4.1 V for poly(135Ph-PZ)-50; and 4.2 V poly(135Ph-PZ)-75 and poly(135Ph-PZ)). Following this, the cell was subjected to equal magnitude and duration discharge pulses and rest cycles until the cell reached the lower voltage cutoff (3.0 V vs Li/Li⁺). The diffusion coefficients were calculated with the following equation:

$$D = \frac{4}{\pi\tau} \left(\frac{n_m V_m}{S} \right)^2 \left(\frac{\Delta E_s}{\Delta E_t} \right)^2$$

where τ is the time of the pulsed current, n_m is the number of moles of active material, V_m is the molar volume of the active material, S is the surface area of the active material, ΔE_s is the change in steady-state potential at the end of subsequent rest periods, and ΔE_t is the change in potential from the applied current pulse, omitting change from iR drop. The V_m of the active material was determined by pressing the active material powder into a pellet and measuring the mass and volume.

Supplemental Figures

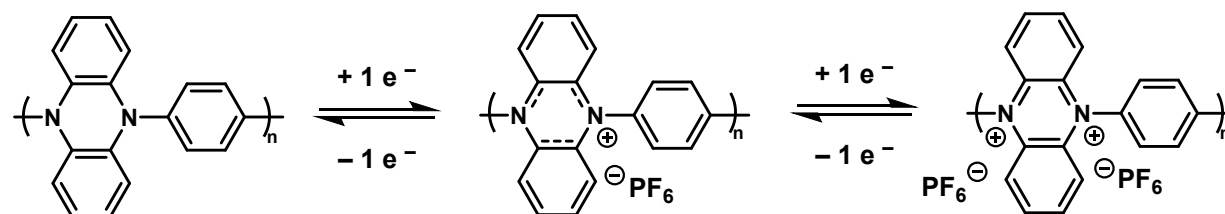


Figure S1. Redox scheme of poly(Ph-PZ).

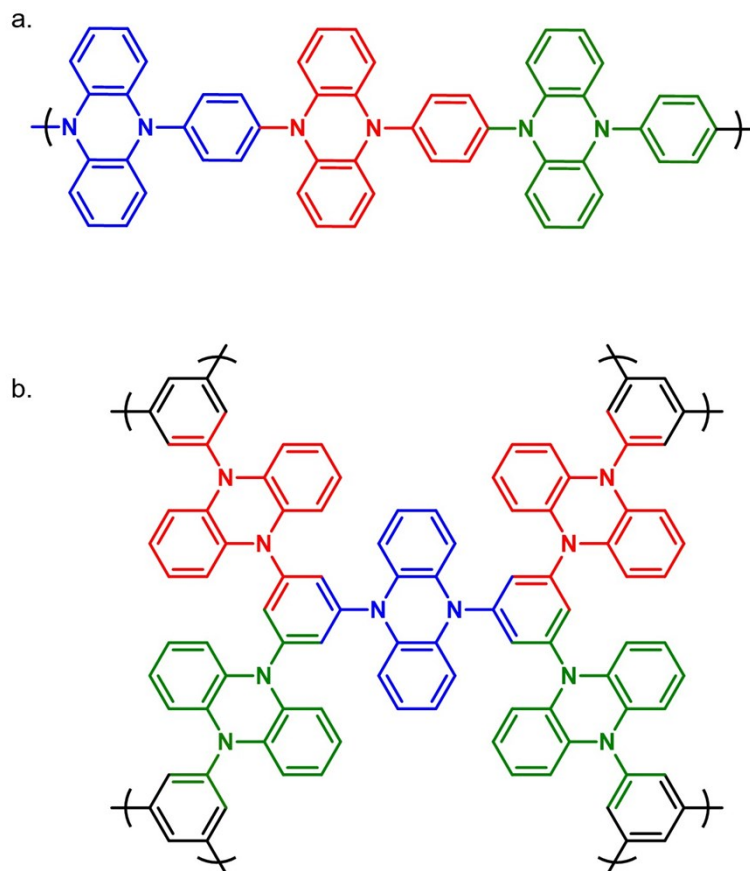


Figure S2. Chemical structures of (a) poly(Ph-PZ) and (b) poly(135Ph-PZ) with the different colors representing the repeat unit used to calculate the theoretical capacity. For poly(Ph-PZ), the repeat unit contains a phenazine unit and a full aryl ring, corresponding to a molecular weight of 256.3 g mol^{-1} and a theoretical capacity of 209 mAh g^{-1} . For poly(135Ph-PZ), the repeat unit contains a phenazine unit and two thirds of an aryl ring, corresponding to a molecular weight of 205.2 g mol^{-1} and a theoretical capacity of 232 mAh g^{-1} .

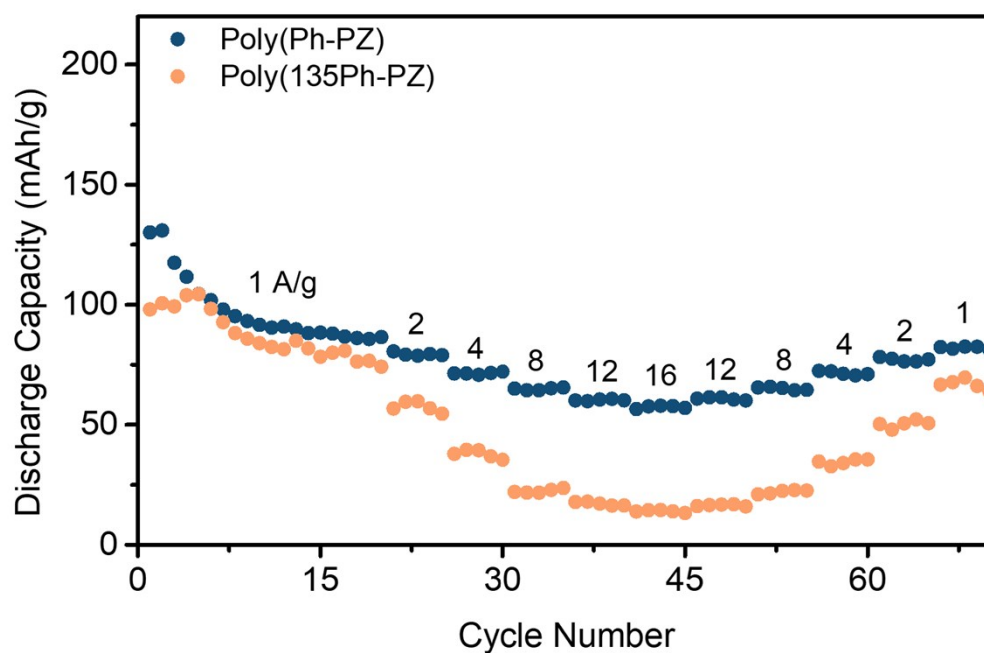


Figure S3. Rate performance of poly(Ph-PZ) (blue) and poly(135Ph-PZ) (orange) in composites containing 80% active material, 10% carbon, and 10% binder, by weight. Cells are charged at 1 A g^{-1} and discharged at the indicated current density.

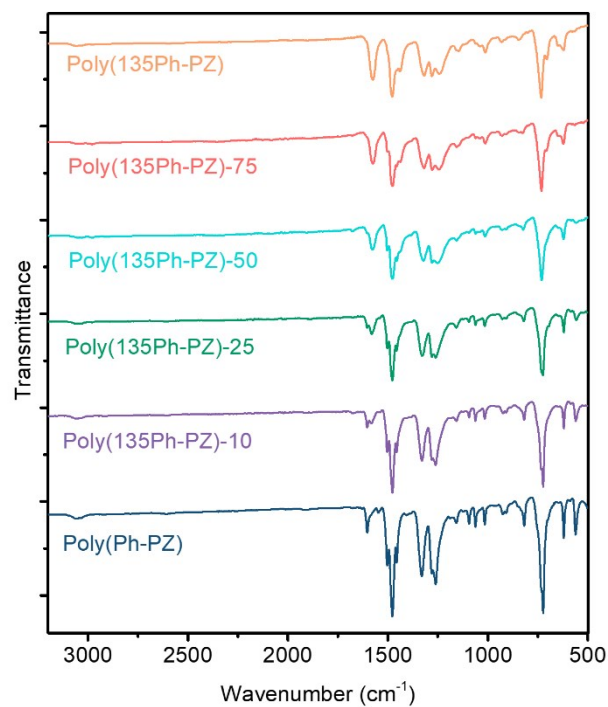


Figure S4. FTIR spectra of the polymers.

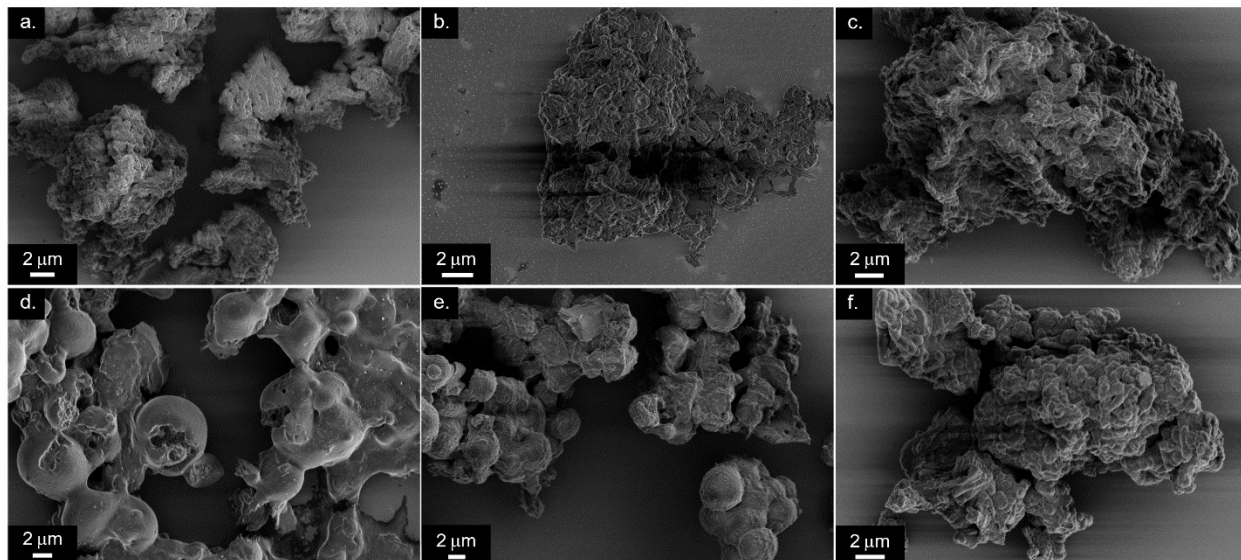


Figure S5. SEM images of (a) poly(Ph-PZ), (b) poly(135Ph-PZ)-10, (c) poly(135Ph-PZ)-25, (d) poly(135Ph-PZ)-50, (e) poly(135Ph-PZ)-75, and (f) poly(135Ph-PZ). To prepare samples for imaging, the polymer powder was dispersed in NMP using sonication and then drop cast onto a clean silicon wafer.

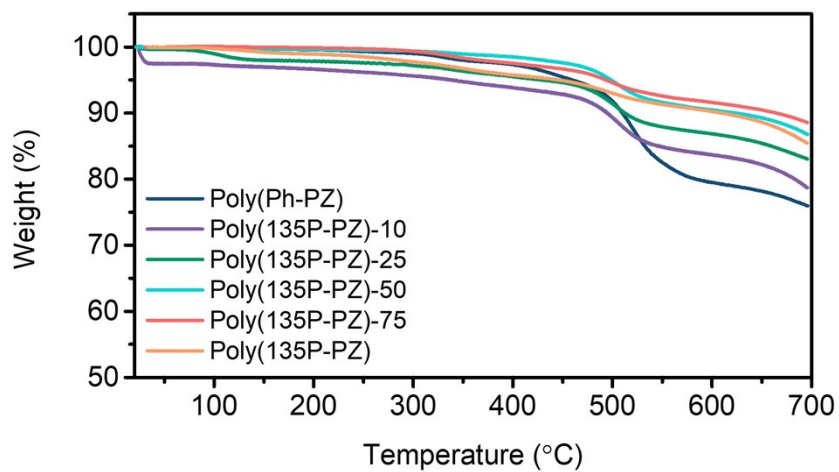


Figure S6. TGA traces corresponding to each of the studied polymers. TGA traces were obtained with a heat rate of $10^{\circ} \text{ min}^{-1}$.

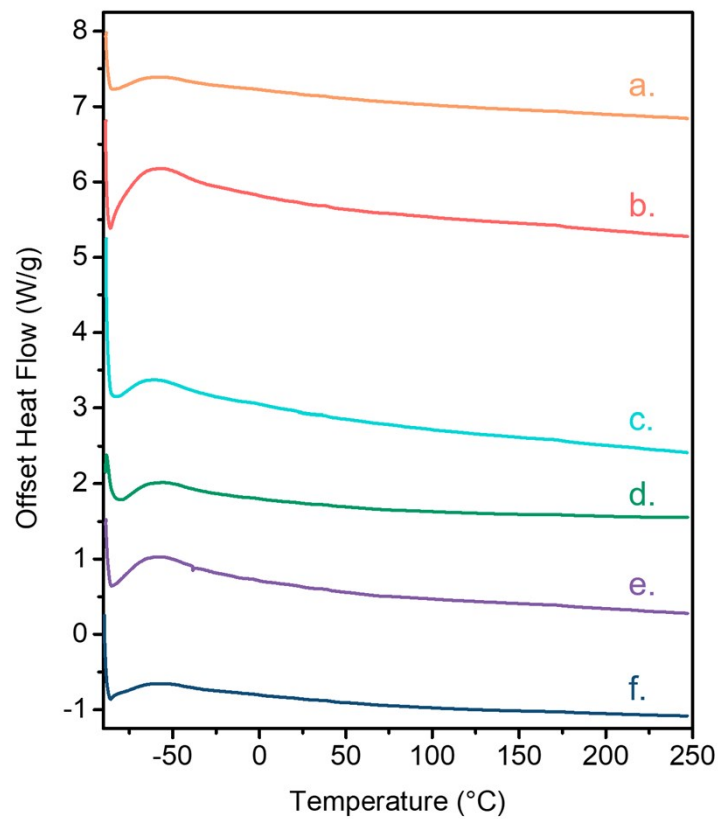


Figure S7. DSC traces of (a) poly(135Ph-PZ), (b) poly(135Ph-PZ)-75, (c) poly(135Ph-PZ)-50, (d) poly(135Ph-PZ)-25, (e) poly(135Ph-PZ)-10, and (f) poly(Ph-PZ).

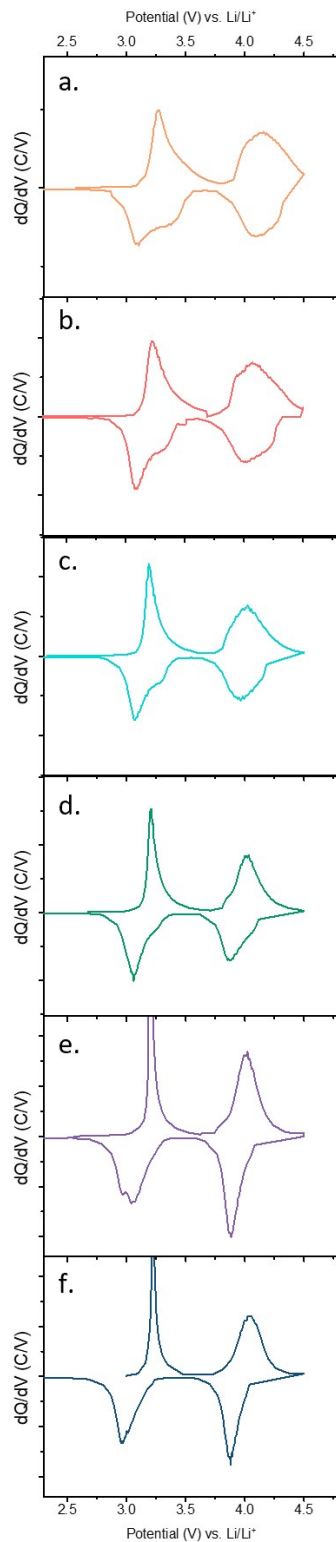


Figure S8. Plots of dQ/dV vs. potential from cycle 20 at 1 A g^{-1} for (a) poly(135Ph-PZ), (b) poly(135Ph-PZ)-75, (c) poly(135Ph-PZ)-50, (d) poly(135Ph-PZ)-25, (e) poly(135Ph-PZ)-10, and (f) poly(Ph-PZ).

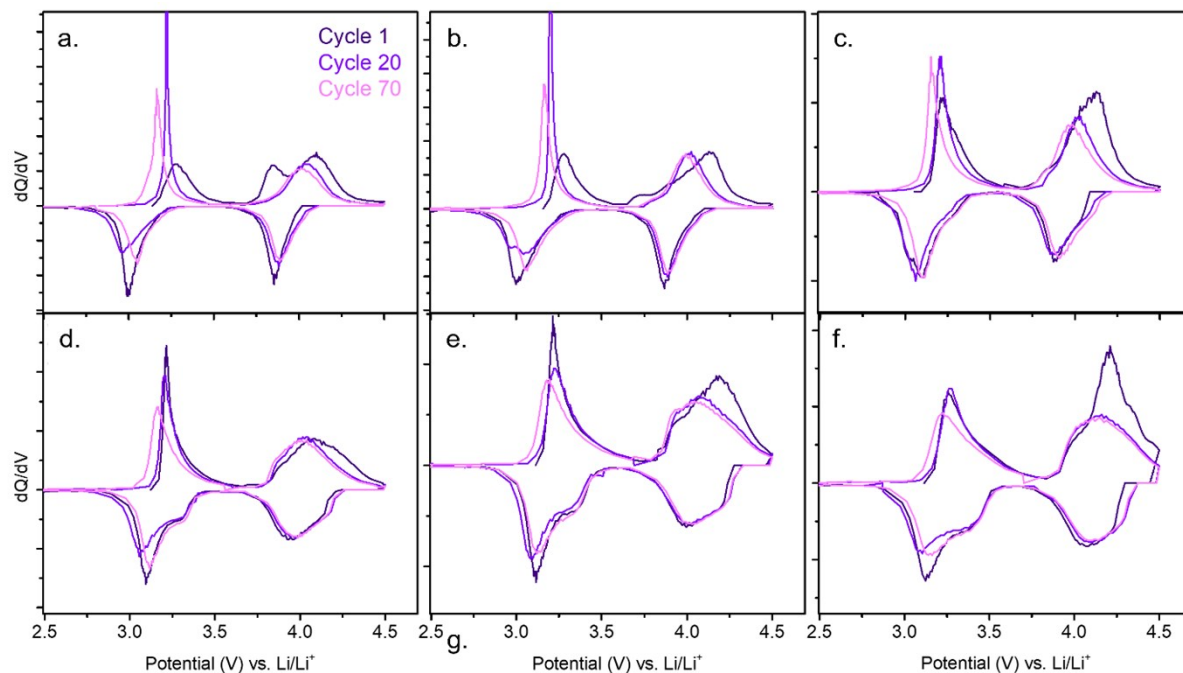


Figure S9. Plots of dQ/dV vs. potential at 1 A g^{-1} from different cycles during rate testing for (a) poly(Ph-PZ), (b) poly(135Ph-PZ)-10, (c) poly(135Ph-PZ)-25, (d) poly(135Ph-PZ)-50, (e) poly(135Ph-PZ)-75, and (f) poly(135Ph-PZ).

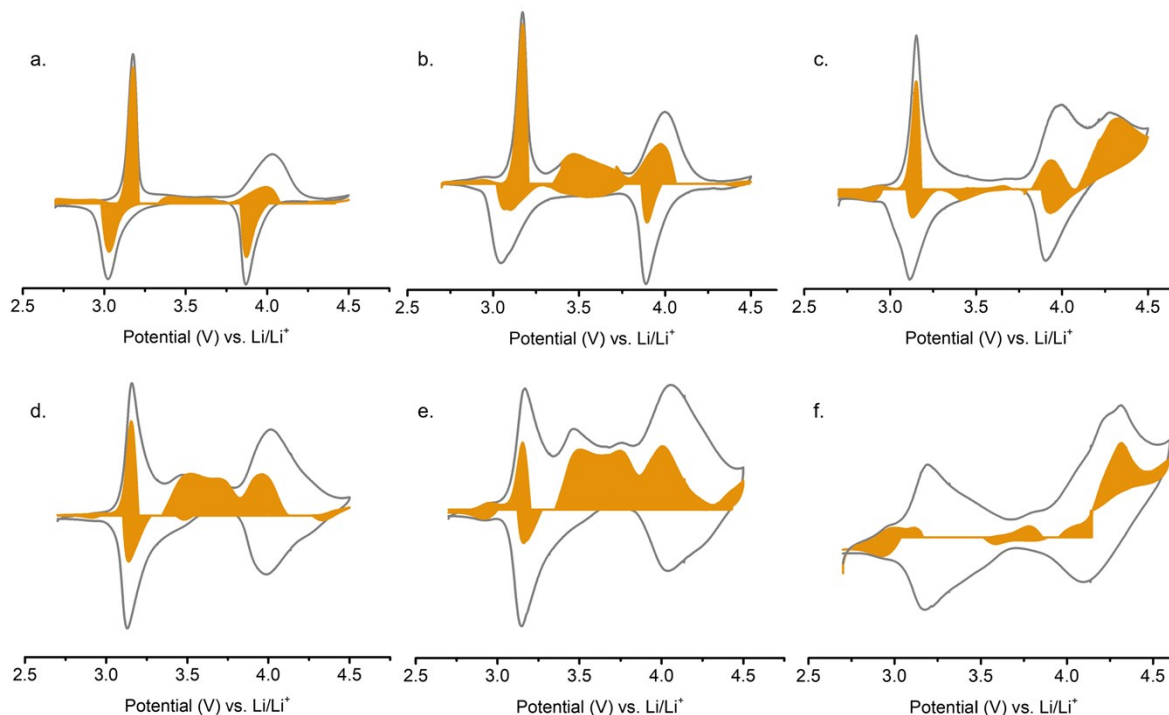


Figure S10. CV profiles at 0.05 mV/s with trace corresponding to the total current in grey and the diffusion limited current determined from Equation 1 in orange for (a) poly(Ph-PZ), (b) poly(135Ph-PZ)-10, (c) poly(135Ph-PZ)-25, (d) poly(135Ph-PZ)-50, (e) poly(135Ph-PZ)-75, (f) poly(135Ph-PZ). At slow sweep rates, additional processes in some cells gave rise to a current response in the anodic sweep, likely a product of kinetically impaired degradation processes at the electrode-electrolyte interface. For

this reason, the cathodic sweep was integrated to determine the percentage of current arising from diffusion limited processes in the polymeric materials.

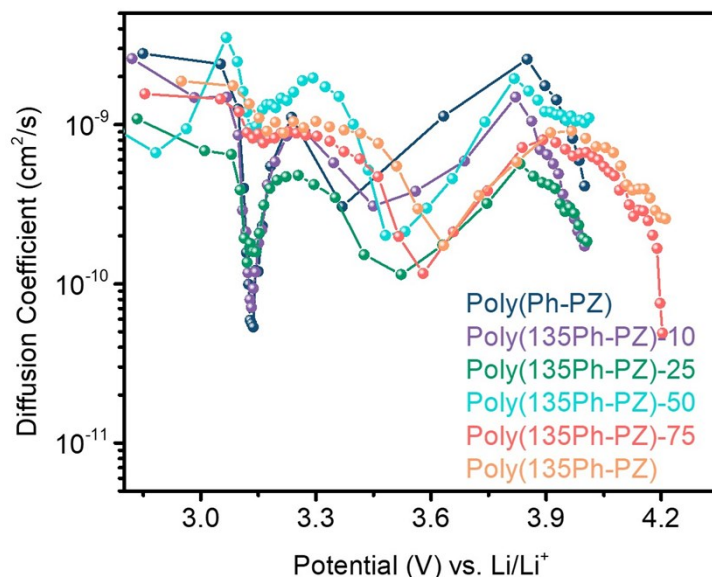


Figure S11. Diffusion coefficients during the charging process determined from GITT.

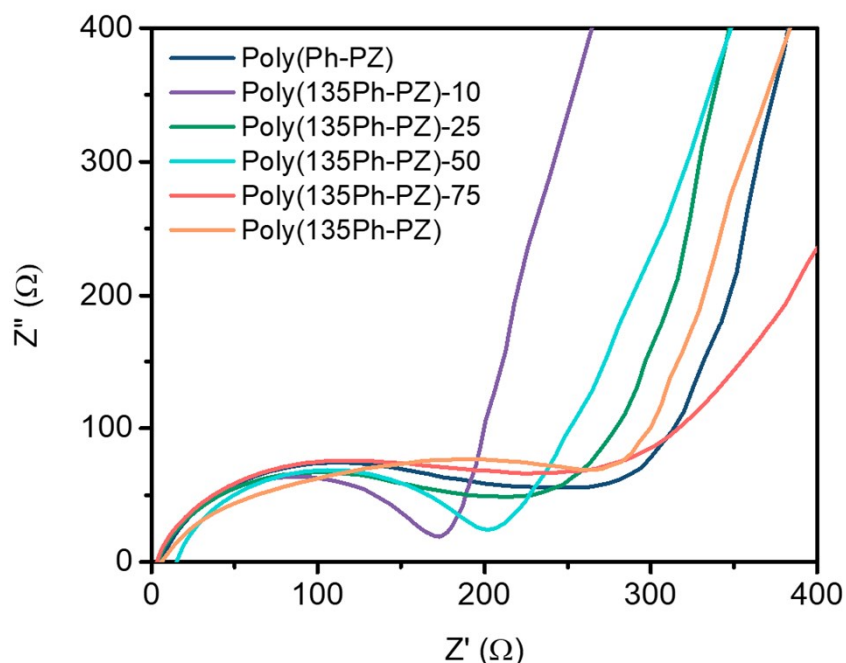


Figure S12. Potentiostatic electrochemical impedance spectra for co- and ter-polymers. Spectra were acquired at 3.6 V vs. Li/Li⁺ during a discharge sweep of the polymers. To ensure the polymers were at steady state, each cell was held at 3.6 V vs. Li/Li⁺ for one hour before the spectra were acquired. The frequency was swept from 50 mHz to 400 kHz using a 5 mV amplitude. 3.6 V vs. Li/Li⁺ was chosen to measure the resistance of partially charged polymers. The potentials where the electron transfer reactions occur were not used to avoid measuring the redox conductivity instead of the electronic conductivity of the polymeric materials.

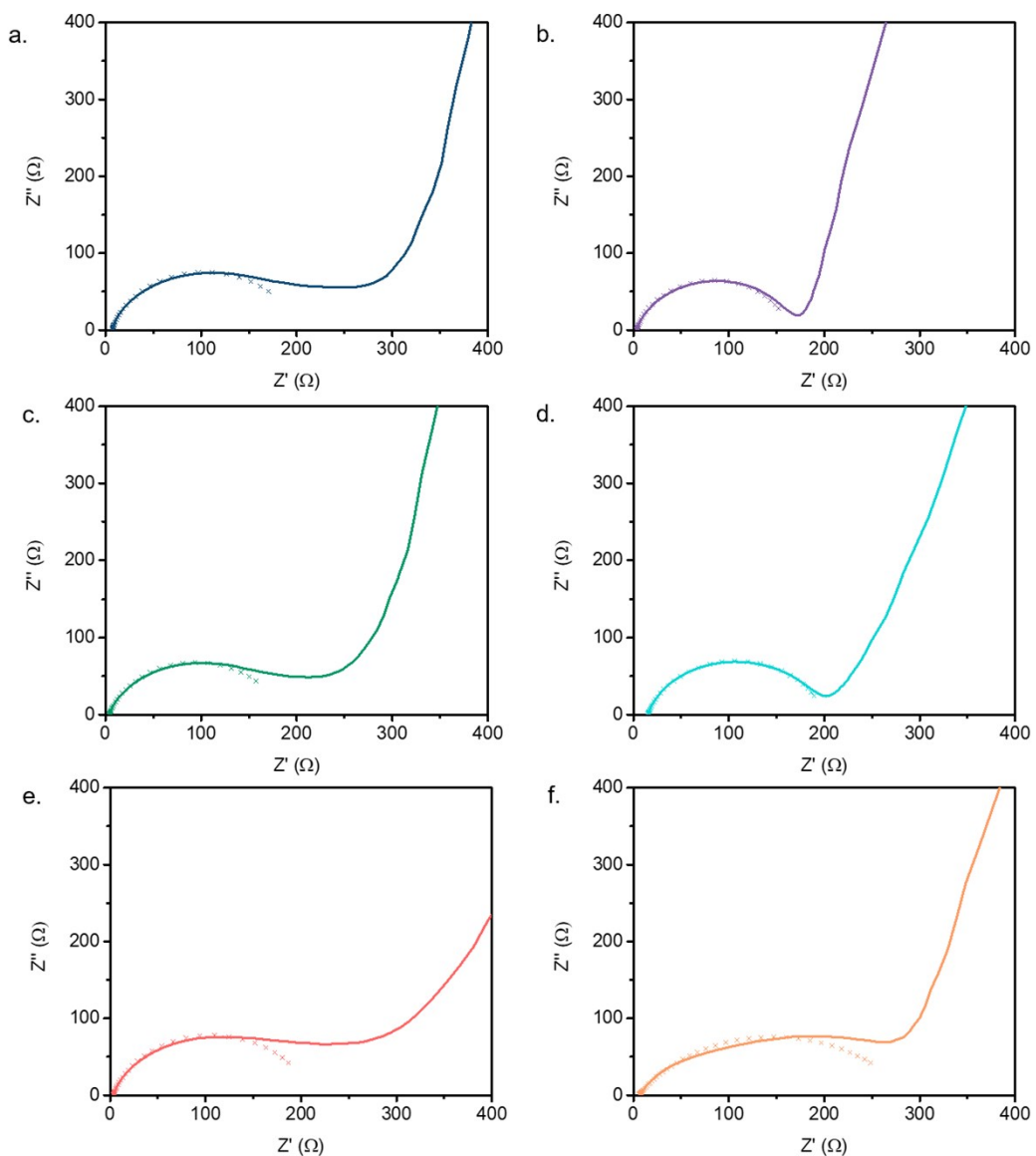
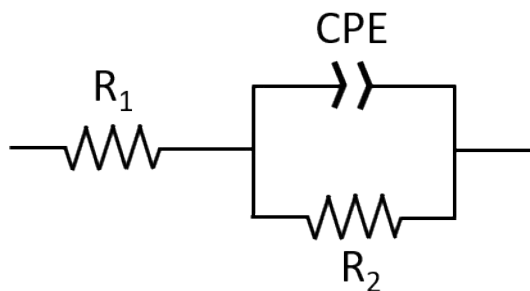


Figure S13. Potentiostatic electrochemical impedance spectra for (a) poly(Ph-PZ), (b) poly(135Ph-PZ)-10, (c) poly(135Ph-PZ)-25, (d) poly(135Ph-PZ)-50, (e) poly(135Ph-PZ)-75, and (f) poly(135Ph-PZ) with fits. Solid lines indicate the experimental data and crosses indicate the fit. EC Lab Z fit software was used to fit the high frequency semicircle to the following circuit:



Where R_1 is the solution resistance, CPE is a constant phase element, and R_2 corresponds to the resistance to transporting charge in the electrode. The fit parameters can be found in Table S1.

Table S1. Fit parameters from impedance spectra in Figure S14.

Polymer	R_1 [Ω]	CPE [$\times 10^{-6}$ F \cdot s $^{(a-1)}$]	a	R_2 [Ω]
Poly(Ph-PZ)	6.6	9.9	0.83	195
Poly(135Ph-PZ)-10	3.5	8.9	0.86	161
Poly(135Ph-PZ)-25	3.9	13.6	0.82	182
Poly(135Ph-PZ)-50	15.1	13.0	0.82	185
Poly(135Ph-PZ)-75	3.2	11.0	0.82	207
Poly(135Ph-PZ)	5.5	96.2	0.63	283

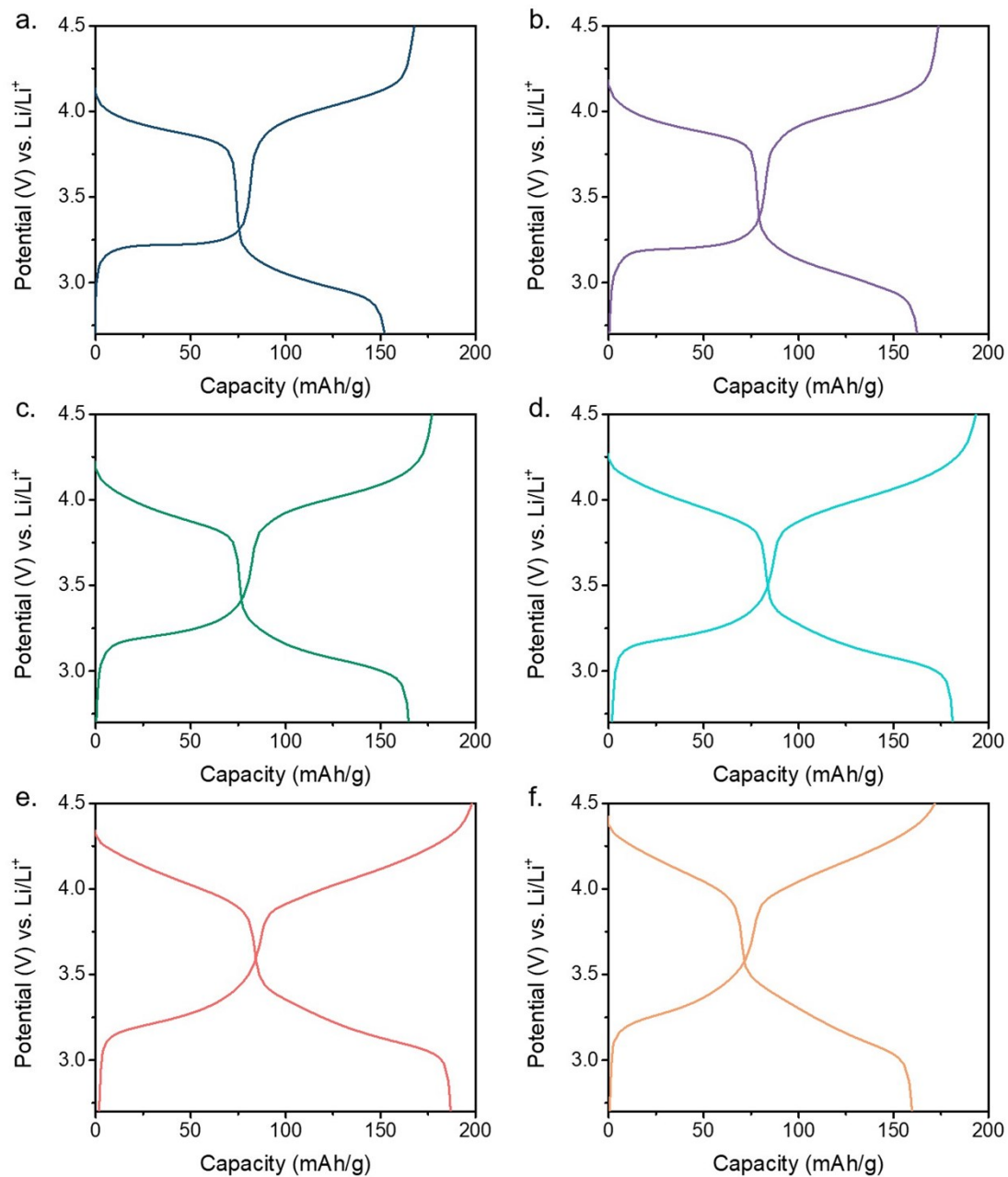


Figure S14. Charge discharge curves from cycle 20 at 1 A g^{-1} for (a) poly(Ph-PZ), (b) poly(135Ph-PZ)-10, (c) poly(135Ph-PZ)-25, (d) poly(135Ph-PZ)-50, (e) poly(135Ph-PZ)-75, and (f) poly(135Ph-PZ).

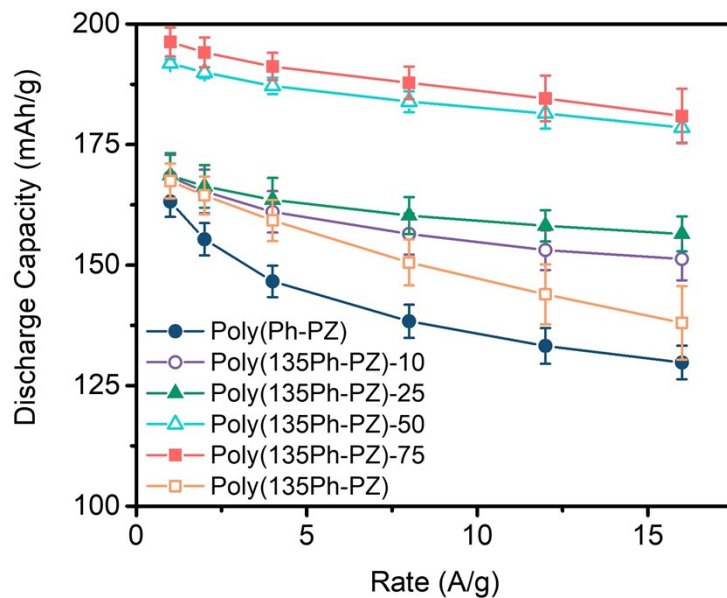


Figure S15. Summarized rate capabilities of polymer composites from Figure 6a. Composites contain 60% active material by weight.

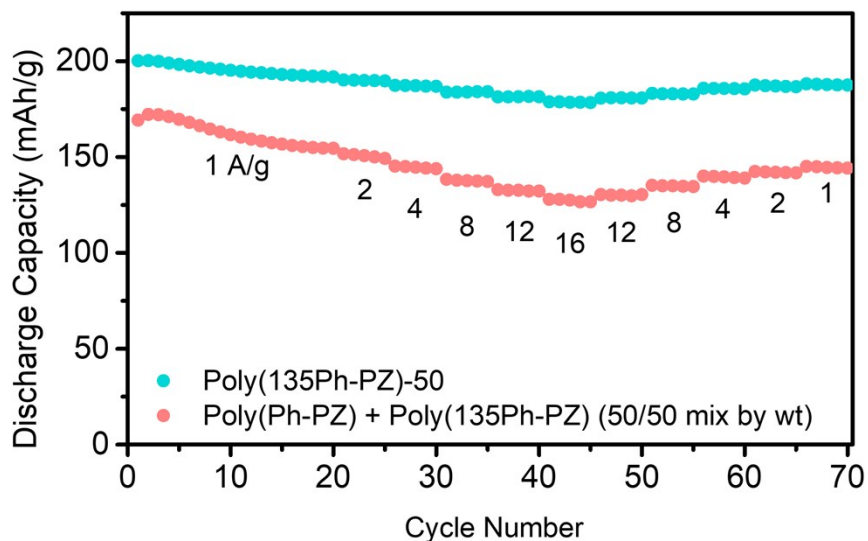


Figure S16. Rate performance of a cathode composite containing 30% poly(Ph-PZ), 30% poly(135Ph-PZ), 30% conductive carbon, and 10% binder, by weight. Rate capabilities are compared to poly(135Ph-PZ)-50 to illustrate the importance of chemically combining species **1**, **2**, and **3** within the same structure to obtain the high capacities and capacity retentions demonstrated by the ter-polymer species in this work.

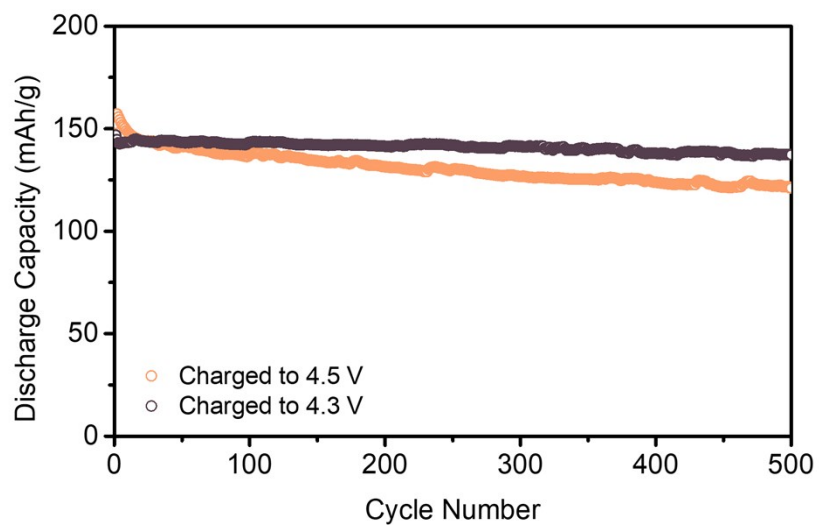


Figure S17. Cells of poly(135Ph-PZ) cycled 500 times at 1 A g^{-1} with an upper cutoff voltage of 4.3 V (brown) and 4.5 V vs. Li/Li^+ (orange).